Climate of the Great Barrier Reef, Queensland

Part 4. Climate change at Rockhampton

Dr. Bill Johnston

Main points

- Climate scientists at the Bureau of Meteorology ignored that the original Stevenson screen at Rockhampton aerodrome was located near the northern boundary behind the Aeradio office. Observations moved to a new, mounded site about 450 m to the south before May 1956 and it seems the effect on data was adjusted using parallel observations that continued possibly until 1963.
- Ignored also was that a satellite communication module (SatCom) installed about 25 m from the second site in 1986 warmed the air sufficiently to cause mean annual maximum temperature (Tmax) to abruptly step-up 0.48°C from 1987.
- Site changes continued after observations transferred to an automatic weather station (AWS) installed on another 1.5 m-high mound in April 1993. The AWS became the primary instrument on 1 November 1996 and tandem manual observations made during that time were apparently destroyed. A 60-litre screen replaced the former 230-litre one on 22 March 2000 and satellite images show that by 13 September 2003 the site became surrounded by bitumen hardstanding that wasn't there in March 1999.
- A step-change in 2013 (0.95°C) was not related to the climate but was due to over-reporting of high-range daily values (values >about 34°C). The change appears to have coincided with the AWS being hard-wired to the Bureau's computers in Melbourne where data were processed into daily maxima, minima and 10-minute and half-hourly observations.
- Although the specific cause of the step-change in 2013 was uncertain, it was unequivocal that the original site moved before 1956 and that the up step in 1987 was related to installation of the SatCom. As neither change was noted, metadata is untrustworthy.
- Adjusted for rainfall, site-related changes caused Tmax to warm 1.44°C overall and after accounting for step-changes and rainfall simultaneously there were no unexplained cycles, changes or trends attributable to the climate.

1. Data sources and background

Daily weather observations for Rockhampton airport (Bureau ID 39083) from 6 August 1939 were downloaded from the Bureau's climate data online facility on 31 January 2020 and summarised into annual datasets using the statistical package R[1]. According to ACORN-SAT metadata[2] "A site move (80 m northeast) took place on 1 April 1993; an automatic weather station was installed at this time and became the primary instrument on 1 November 1996". Site summary metadata (27 July 2018) locates the original Aeradio site at Latitude -23.3753° Longitude 150.4775°, which are the coordinates of the current site, while a 2012 weather station list (http://www.bom.gov.au/climate/how/newproducts/images/cr_sites_alpha.txt) placed it

---

[1] https://www.r-project.org/

[2] Australian Climate Observations Reference Network – Surface Air Temperature (ACORN-SAT) Station catalogue (p. 89 of 120 pp.) (http://www.bom.gov.au/climate/change/acorn-sat/documents/ACORN-SAT-Station-Catalogue-2012-WEB.pdf)

beside a taxiway linking with the new terminal (Latitude -23.3769°, Longitude 150.4761°), which was also in error.

Metadata ignored that the 1939 Aeradio office with its 60-foot (18 m) roof-mounted anemometer was on the northwestern side of the airport and that the instrument enclosure was near the aerodrome's northern boundary[1] (Appendix 1). Also, a 1944 plan shows the United States Weather Bureau occupied an adjacent separate office and store (NAA Barcodes 6678275 and 6678276). A May 1956 aerial photograph (Figure 1) shows extended runways and aprons in preparation for construction of a new terminal/control tower on the eastern side of the runways, which opened in 1961; while the close-up view of the same image shows the met-enclosure linked to the Aeradio office by a concrete path (Figure 2). A new site ("X" in Figure 1) was also operational in 1956 about 450 m south of the original one. According to Wikipedia WWII demolition tunnels under the runways were located and filled during upgrade work in 1987[2].

Google Earth Pro satellite images (Figure 3) shows that about 15 ha of former grassland south of the site became occupied by buildings, hardstanding and parking areas before September 2003.

Figure 1. By May 1956 former WWII runways had been lengthened and strengthened and a new taxiway and apron for the new control tower and terminal were under construction on the southern side of the airport. Identifiable WWII-era buildings (right) were (1) control tower and signal square; (2), terminal; (3), hanger; (4), Aeradio/met office with hydrogen generator shed behind; (5), RAAF barracks; (6), powerhouse; (7), met enclosure; (8) USAF garrison and barracks and (9) armoury. 'X' marks location of the new site. The building at (10) appears to be a site office or possibly a temporary met or radio-aids office. (Portion of a State of Queensland aerial photograph[3] QAP0616020 (Ridgelands Run 5 Print 616-20; 29 May 1956). The track linking (10) with the new site (X) and the previous Aeradio site suggests they operated in parallel for several years.

[1] National Archives of Australia (NAA) Barcode 1724071 and 1724277. (Search barcodes at: http://soda.naa.gov.au/barcode/)

[2] https://en.wikipedia.org/wiki/Rockhampton_Airport

[3] Queensland aerial photographs (prefixed QAP) were obtained from QImagery (https://qimagery.information.qld.gov.au/)

In 1986, prior to local air traffic control (Flight Services) being withdrawn in 1992, satellite communication equipment (SatCom)[1] was installed in close proximity to the second site, which was mounded about 1.2 m above the natural ground surface. While the heat-emitting electronics cabinet warmed the data from 1987, the Stevenson screen was not moved to its current 1.5 m-high mound until 1st April 1993. There was no apparent change in Tmax caused by the move.

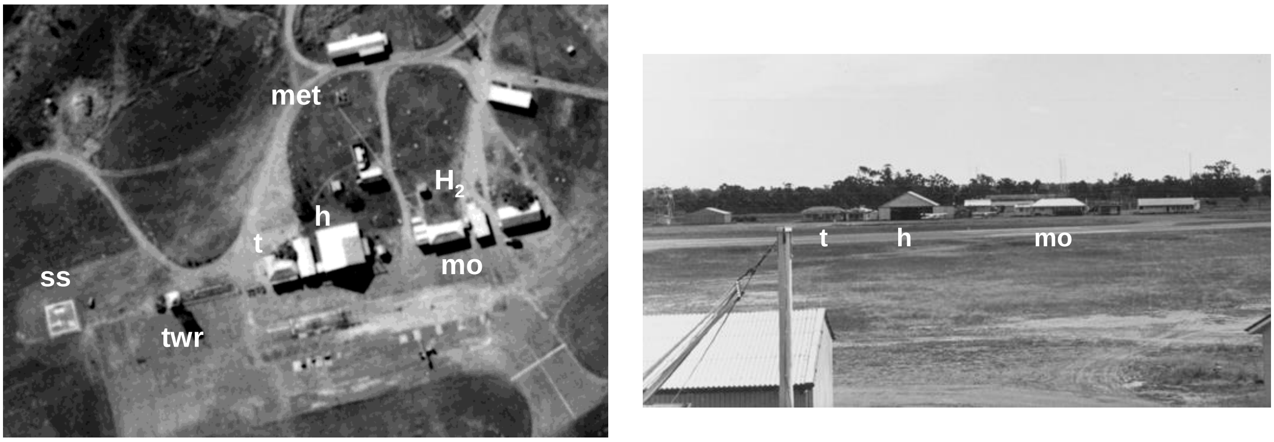

Figure 2. A close-up view of the airport operations precinct in 1956 shows the met-enclosure in the same position as it was in 1939 (Appendix 1) and a concrete path leading from the then Aeradio-met office (mo). The shed behind the office (H_2) was probably the hydrogen-generator for filling balloons used to estimate windspeed and direction. Other buildings included the control tower (twr) and signal square (ss), terminal (t) and the pre-WWII hanger (h). The airside view (right) was taken later from the new control tower with the fire station in the foreground.

Figure 3. Rockhampton airport during the 1991 flood (left) showing location of the second met-enclosure (S_2) atop a mound about 25 m from the heat-emitting SatCom (S/C) equipment (portion of QAP4925078, 14 January 1991); and right, portion of Google Earth Pro satellite image (20 June 2010) showing changes in the vicinity of the former operations precinct (h is the pre-WWII hanger but other buildings had been demolished), expansion of hardstanding areas, the new mounded site (S_3), which operated from 1 April 1993, and the new 1990s met-office (mo).

---

[1] SatCom ground stations and associated heat emitting electrical cabinets were installed at 94 airports across Australia in 1986/87

Despite constant assurances by Bureau scientists that site histories of 'high quality' ACORN-SAT site have been carefully researched, metadata is faulty and deficient. Maps, plans and aerial photographs unequivocally show the original site was north of the Aeradio office (at about Latitude -23.3722, Longitude 150.4757) and that it moved south of the runway before 1956. The changed aspect and exposure of the new site would most certainly have affected the data but it appears differences were smoothed or adjusted-out using overlap observations. Later changes including installation of satellite communication equipment, new taxiways, hardstanding and air-conditioned terminal buildings (Figure 3) were ignored to imply effects were due to the climate.

2. Analysis of maximum temperature

As the effect of possible temperature extremes and climate change on the Great Barrier Reef is of primary interest, only maximum temperature (Tmax) was analysed in detail for this study (the dataset is available in Appendix 2).

2.1 Methods

Following similar procedures to those outlined for Gladstone Radar, naïve linear regression was used to evaluate the relationship between Tmax and rainfall and partition the effect of rainfall on Tmax from that due to non-rainfall factors[1]. Homogeneity of residuals was evaluated using an independent statistical test of the null hypothesis that the mean was constant, Step-change scenarios identified using categorical variables were compared using multiple linear regression (MLR) with rainfall as the covariate. Covariate-domain analysis of pooled data is versatile, statistically powerful and robust and adopting the same rules as outlined for Gladstone, the outcome could not be pre-determined.

Raw data-segments and MLR-residuals were tested for trend and change in the time-domain to verify appropriateness of the step-change model and as data and statistical tools are in the public domain, analysis is replicable.

2.2 Results

2.2.1 Covariate domain analysis

Ignoring outliers (which were identified separately), rainfall naïvely reduced Tmax 0.124^{o}C/100 mm (Figure 4(a)); P <0.001 and explained 28.6% of Tmax variation (R^2_{adj} = 0.286). Variation that was *not* explained included random synoptic or clustered effects related to the El Niño southern oscillation; inaccuracies, instrument faults etc. that may affect precision of observations; and changes (or shifts) in conditions affecting observations such as instrument changes, relocating to different exposures, changes in the environment being monitored or site specific issues including cessation of regular maintenance.

To aid interpretation, zero-centred residuals were re-scaled by adding grand-mean Tmax (28.42^{o}) before undertaking step-change analysis (Figure 4(b)). As the procedure is objective and replicable, results could not be determined in advance. Also, had the naïve Tmax ~ Rainfall relationship fully explained the data, residuals would be random, normally distributed, free of step-changes and other systematic signals and analysis would be complete.

Step-changes or shifts in the re-scaled mean identified discontinuities in the data-stream that were unrelated to rainfall, and inhomogeneties as small as ± 0.3^{o}C, which approximates the uncertainty of comparing two observations may be detectable. Changepoints may also be confirmed *ad hoc* using parametric or non-parametric 1-way analysis of variance with data segments specified as 'blocks'.

---

[1] Observed data (Tmax through time) consists potentially of several overlaid signals, namely: (i), deterministic variation caused by rainfall (Tmax depends on rainfall in a physical, thermodynamic sense); (ii), non-random underlying systematic variation and; (iii), the remainder, which is random. Accounting for the deterministic rainfall portion using linear regression provides a 'drill-down' approach to detecting signals that are not rainfall related.

Segmented free-fit regressions (Figure 4(c) to (e)) show relationships were offset relative to long-term median rainfall (747 mm) and mean-Tmax (28.4°C) and slopes were likely to be parallel. However, while slope coefficients were significant and variation explained (R^2_{adj}) varied from 0.39 to 0.73, individual regressions were unable to be compared except by analysing the composite dataset simultaneously.

Multiple linear regression of the pooled dataset (Figure 4(f)) confirmed that: (i), rainfall-adjusted segment means were different (segmented regressions were not coincident and step-changes were not due to persistent changes in rainfall); (ii), rainfall reduced Tmax 0.108°C/100 mm overall; and, (iii), as interaction[1] was not significant (P = 0.55) response to rainfall was the same across segments (Figure 4(d)). Accounting for site changes and rainfall simultaneously, increased variation explained from 28.6% (Figure 4(a)) to 69.7% (Figure 4(d)). Subsidiary analysis (not shown) also identified that data for 1973, 1989, 2009 and 2012 were outliers.

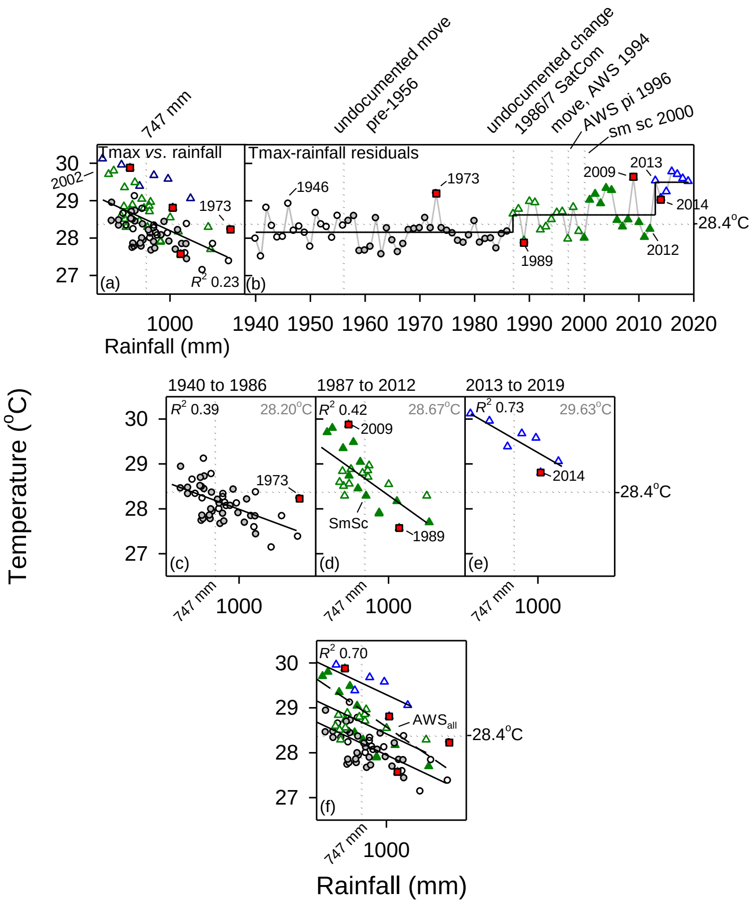

Figure 4. As the naïve case (a) did not account for underlying inhomogeneties, rainfall alone explained only 22.7% of overall variation in Tmax. Inhomogeneties (step-changes) in (b) were aligned with known or suspected site changes *post hoc*. Although the site moved from near the northern boundary of the airport before 1956 the effect of the move was apparently adjusted-out of Tmax data. While the step-change in 1987 aligned with installation of a satellite communications module within 25 m of the site, the change in 2013 was not attributable to a site change. Segmented analysis ((c) to (e)) showed regression lines were offset relative to median rainfall (747 mm) and average Tmax (28.4°C); rainfall adjusted values (grey font) were different, lines were parallel (f), and rainfall and step-changes together explained 70% of Tmax variation. Response to rainfall by AWS data from 1996 (dashed line in (f)) cuts across two segments and is biased-high.

Finally, while time-domain raw-data trends from 1940 to 1986 and 1987 to 2012 were not significant, a quasi-linear decline in rainfall from about 2013 to 2019 resulted in a commensurate increase in Tmax. Although removing the effect of rainfall reduced that Tmax trend to zero, the step-change remained embedded in the non-rainfall portion of the signal.

[1] Specified as: Tmax ~ Sh_{factor} * rainfall

Covariate-domain MLR residuals were normally distributed, homoscedastic (equal variance across categories) and independent and as no residual systematic signals were detectable, no trend or change was attributable to the climate or any other factor.

Step-change analysis of the residual, non-rainfall portion of the Tmax signal was confirmed by covariate analysis and where possible cross-referenced by metadata, aerial photographs and ancillary information. However, evidence linking the 2013 up-step to site changes was lacking. In addition, aside from the effects of drought on surrounding vegetation, no noticeable changes were evident in successive Google Earth Pro satellite images of the site. On the other hand the shift was clear and abrupt, highly significant, unrelated to rainfall and not a trend (rainfall-adjusted delta-T = 0.96^{o}C, P <0.001).

Ignoring outliers, the relationship between Tmax and rainfall for the homogeneous 46-year segment to 1986 (shown in Figure 4(b) and Figure 4(c)) was used to predict Tmax for the subsequent 33-years from 1987 to 2019. Had site conditions, observing practices and other factors remained the same, observed data were expected to vary within the bounds of 95% prediction intervals (Figure 5). Although due to the step-change, Tmax was mostly warmer than predictions; clustered out-of-range values evident after the small Stevenson screen was installed in March 2000 and especially from 2012 warranted further investigation.

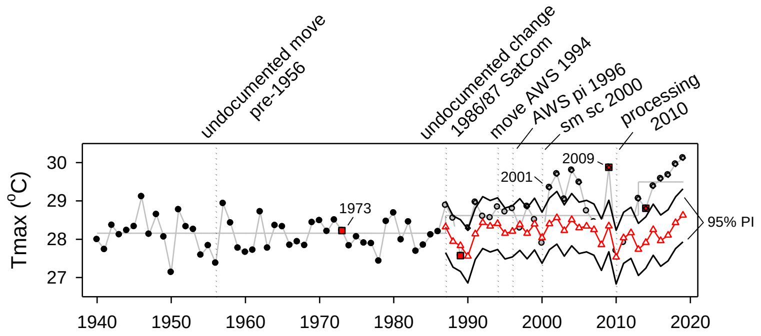

Figure 5. The relationship between Tmax and rainfall for the homogeneous 47-year segment prior to the 1987 SatCom step-change (dark circles) was used to predict Tmax for the remaining 33-years to the end of the record (open red squares). Post-1987 data (grey circles) greater than the 95% prediction interval were out-of-range. (While the prediction equation ignored data for 1973, data for 2009 was spuriously high.)

Below average rainfall from about 1991 (Figure 6) resulted in a dry epoch lasting until 2007 (17 years) which was the longest period of below-average rainfall since 1940 and therefore of predictably-higher Tmax. The situation reversed from 2010 to about 2016, after which dry conditions again prevailed; however, relative to predictions, as Tmax increased quasi-linearly from 2010 (Figure 5) it appears that some process or instrument fault disrupted the Tmax ~ rainfall relationship.

2.2.2 Frequency domain analysis

Counts of observations per year greater than (less than) the 95th (5th) day-of-year percentiles define spread in the tails of the distribution of daily values. Although frequencies may vary in response to clusters of wet and dry years, unless other factors intervene they are expected to be random overall.

Before 1956, counts of daily values <5th percentile (Lo-extremes) were higher than those >95th percentile (Hi-extremes), indicating the original site was relatively but not markedly cool (Figure 7) i.e. while not sufficiently cool to affect mean-Tmax, environs may have been watered for instance. After the site moved effects of wet years in 1968, 1973 and 1978 were short-lived and although the new site was somewhat cool, frequencies were random until the SatCom was installed and counts of Hi-extremes stepped-up permanently.

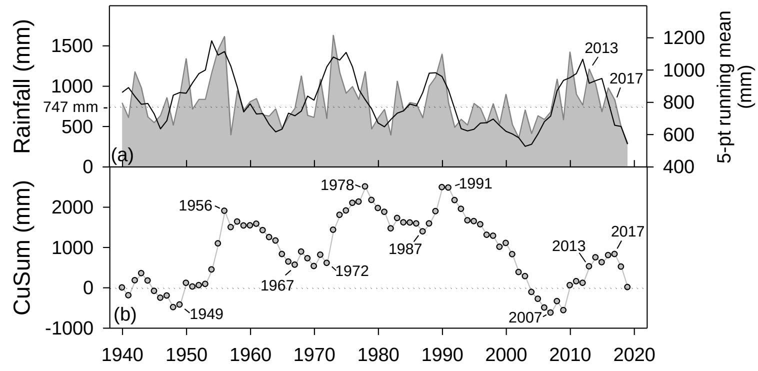

Figure 6. Highlighted by the 5-point running mean (right axis in (a)), annual rainfall consisted of episodes of dry years interspersed about every 20 years or so by clustered wet years. Median rainfall is indicated by the dotted line. The cumulative sum of deviations from the mean (CuSum) shows periods when rainfall is cumulatively above average (the curve ascends), below average (it declines) or about average (horizontal). Thus from peaks in 1956, 1978, 1991 and 2017 rainfall was cumulatively less than the mean and vice-versa from troughs in 1949, 1972, 1987 and 2007. Towards the end of the low-rainfall epoch to 2007 the district experienced severe drought.

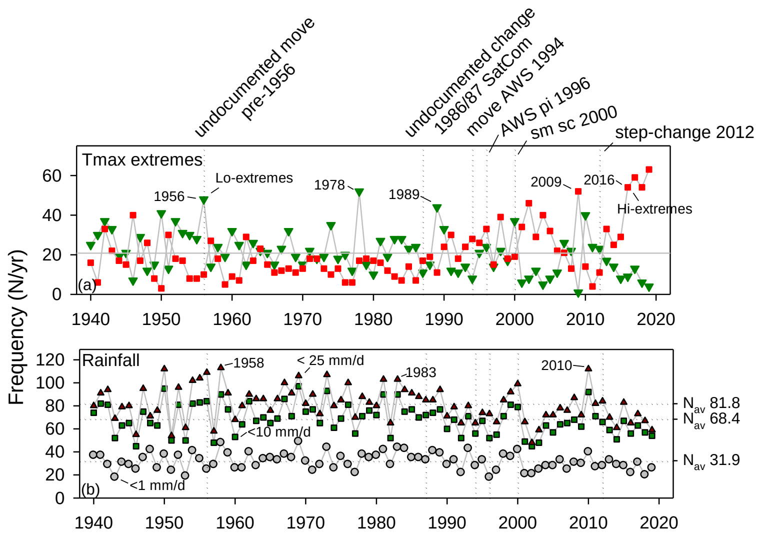

Figure 7. Frequency (counts/yr) of Tmax observations greater than (squares) and less than (inverted triangles) the 95th and 5th day-of-year percentiles (a) and the frequency of daily rainfall within classes (<1 mm/d, <10 mm/d and <25 mm/d) were expected to be random overall.

As variation due to rainfall is confounded with potential inhomogeneties and both are potentially influential, inferences based on raw data alone may be compromised. For instance the numbers of rain-days >25 mm/d declined from 1983 (Figure 7(b)) and following a brief respite from 1994, frequency of all rainfall classes stepped-down abruptly in 2000. As rainfall is neither random nor stable, attribution of Tmax frequency changes to either site changes or the climate is problematic.

Applying the same approach to that used previously (Figure 5), naïve linear regression partitioned frequency data (and their ratio) into rainfall-related components and residuals that potentially embed site-related inhomogeneties. Thus, while effects on frequencies were confounded in Figure 7, in Figure 8 rainfall-related variance was removed. Step-changes in residuals (Figure 8 (d) to (f)) were therefore due to factors related to the data not the climate.

Although the step-change in 2013 was confirmed as significant, the previously undiscovered change in 1990/91 was not aligned with known factors (Figure 8(e)). Time-wise error is a possibility - a non-parametric CuSum-based test found with 95% confidence that the 1990 changepoint occurred between 1986 and 1995 and that Tmax variation increased after 1996 when the AWS became the primary instrument. Further, 1994 and 1999 aerial photographs showed the new site bereft of groundcover, which irrespective of other factors, would cause it to be warmer on warm days.

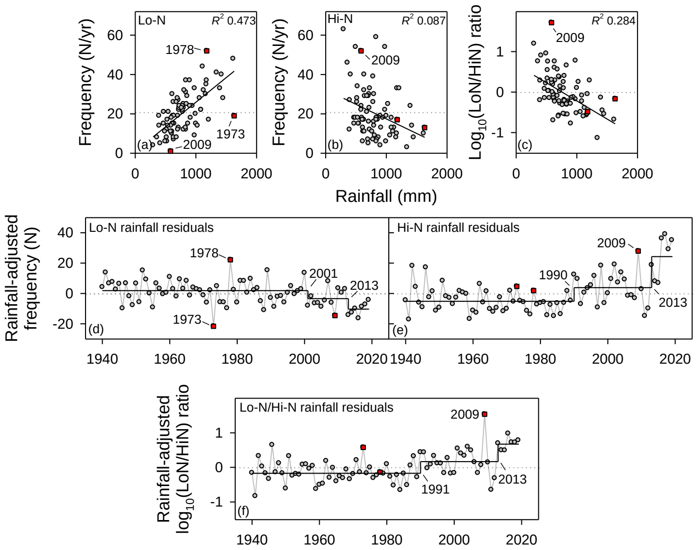

Figure 8. Effects of rainfall on the frequency of daily Tmax <5th (Lo-N) and >95th day of year percentiles ((a) and (b)) and their (Lo/Hi) ratios (c) and rainfall-adjusted sequences showing step-changes in respective zero-centred means. Data for 1973, 1978 and 2009 were identified as outliers (infilled red squares). As variance was related to rainfall ((a) to (c)), further analysis (not shown here) required data to be transformed to logarithms.

Exploring the problem further, probability density functions of daily Tmax and minimum temperature (Tmin), and percentile differences, calculated for equi-length segments straddling the 2013 changepoint (1 January 2006 to 31 December 2012 *vs*. 1 January 2013 to 31 December 2009) for Rockhampton and the AWS at Yeppoon (Bureau ID 33294; 38.7 km distant) were compared. Data-days per tranche were similar (N = 2458 to 2557) and both sites were automated and used 60-litre Stevenson screens.

Probability density functions show the relative likelihood that values of a continuous variable fall within particular data-ranges. Thus density or likelihood is highest around the mean, mode or median and is axiomatically less toward the tails (Figure 9). As areas under curves is unity and Tmax and Tmin distributions were each calculated across identical x-axis ranges, respective pairs of curves are comparable. Thus, while peak Tmax density for Yeppoon was higher than Rockhampton, tails of the distribution were narrower.

While probability density functions visualise the *shape* of data distributions they provide limited insights into the *nature* of the changes, which may be due to: (i), a constant offset across the percentile range (pre *vs*. post percentiles displace vertically); (ii), tails become radically different due to atypical outliers, while means/medians are unchanged; (iii), across-range differences, are related to values being measured (one or both tails of the distribution are affected); or (iv), random imbalances of values less than/higher than dataset medians (patchy or incoherent differences). For instance at Yeppoon, while Tmin differences were inconsistent/random, low-range Tmax (<25.9^{o}C) shifted warmer while except for several outliers, post-change upper-quartile values were about the same.

It is highly improbable that post-2013 daily Tmax greater than the median could increase quasi-linearly at Rockhampton, to 1 to 2^{o}C warmer above the 90th percentile, without a corresponding increase in either Yeppoon Tmax or Rockhampton Tmin (Figure 9) and equally unlikely that while Tmax increased, lower-range Tmin shifted from being >1^{o}C warmer to cooler across it's percentile range. Something happened – the instrument became faulty and was not replaced;

1-second sample values regularly over-ranged the calibration or data were manipulated to be warmer than they were. Given that both tails of Tmin and Tmax were compared and the comparison extended to the nearby site at Yeppoon, there is no other possible explanation.

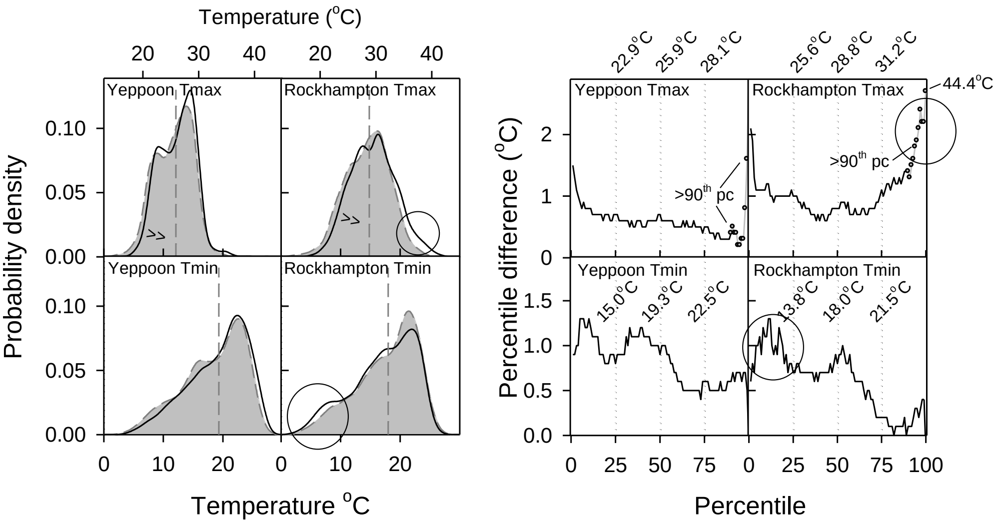

Figure 9. Left: Pre-2013 Tmax and Tmin probability density functions (shaded) compared with post-2013 distributions for Yeppoon and Rockhampton. Dashed vertical lines reference pre-2013 median temperatures, which are the same as 50th percentile values on the right. The right panel shows changes in paired distributions as percentile differences (post-2013 minus pre-2013). The main change in the Tmax distribution at Yeppoon was due to higher daily values in the less-than 1st quartile (22.9^{o}C) band, whereas at Rockhampton the shift was due to data shifting-up generally by about 1^{o}C, and those >3rd quartile becoming 1 to 2^{o}C warmer. (Tmax values >90th percentiles (29.5^{o}C for Yeppoon and 33.4^{o}C for Rockhampton) are highlighted.) Highest post-2013 Tmax at Rockhampton (44.4^{o}C on 28 November 2018) was estimated to be 2.7^{o}C over-range.

3. Discussion and conclusions

Covariate analysis circumvents the problem of isolating the 'true' Tmax signal from underlying inhomogeneties that affect trend and change. For instance naïve analysis of Rockhampton Tmax, say using Excel, assumes *a priori* that trend is a property of the signal alone and is not impacted by non-climate factors. While the assumption that data are homogeneous is the most commonly ignored issue in time-series analysis, covariate analysis provides the most convenient and established methodology for assessing that data are fit for purpose.

The three-step procedure involves: (i), use of naïve linear regression to partition total variation in the signal of interest (Tmax) into that attributable to the covariate (rainfall) and that which is unexplained (residuals); (ii), independently test the null hypothesis that the cumulated mean of residuals is constant and identify data-segments whose means are the same using indicator or dummy variables; (iii), verification that covariate-adjusted segment means are different (individual regressions are not coincident); and that interaction between categories and the covariate are not significant (i.e. slopes are homogeneous) using multiple linear regression.

The approach is straightforward, not controversial and used in many disciplines, including medical and econometric sciences where classificatory variables aid understanding of the response to an independent variable. Pooling data improves the likelihood of detecting meaningful category differences, while the rules-based framework outlined previously ensures exclusion of mis-specified breakpoints.

The Bureau of Meteorology's handing of data, metadata and the conduct of their long-running climate experiment is called into question by the analysis. It's impossible that the pre-1956 move revealed by aerial photographs and supporting documents was not recorded in Bureau files. It required negotiation with the Royal Australian Air Force or Department of Civil Aviation;

approvals of expenditure at Director level; requisitions to the Department of Public Works (Cwth) for building the mound and installing equipment. It may have taken months to complete after which parallel observations were made for a further three or more years. Adding to the debacle, it appears the data were changed to hide the move, which further undermines trust in the Bureau's processes.

It is also not possible that observers were unaware that the SatCom was installed 20 to 30 m from the site probably in 1986, or that the heat from the electronics cabinet affected measurements. Also perverse is that the 1987 step-change, which was highly significant in both time and rainfall domains was not detected or adjusted by data homogenisation. For example, raw-Tmax trend to 1986 was -0.023^{o}C/decade; ignoring the step-change it increased to 0.131^{o}C/decade to 2010 and 0.152^{o}C/decade to 2019. Satellite images (Figure 10) show site changes have been on going.

Despite at least four homogenisation iterations of the same data and repeated assurances that the history of the site had been exhaustively researched, failure to detect and adjust the 1987 step-change exposed a major weakness in the Bureau's homogenisation methods; namely, that the process lacks scientific objectively and oversight; adjustments applied arbitrarily can result in pre-determined or biased outcomes; and, that at all levels (publications in scientific journals; books; bulletins; in-house and by 'independent' reviewers), the peer-review process failed dismally .

Multiple analyses of the 2013 step-change found it was due to either an instrument fault or off-site data processing, not the climate. The change was independent of rainfall (Figure 4(b)); data were increasingly off-scale relative to predictions (Figure 5); and although rainfall in 2019 was the lowest since 1940, the developing drought was not especially harsh (Figure 6). Step-changes also persisted after the effect of rainfall on counts of upper and lower extremes and their ratio was removed (Figure 8). Finally, probability density functions and percentile differences (Figure 9) showed that in contrast to Tmax and Tmin at Yeppoon and Tmin at Rockhampton, daily Tmax values >90th percentile were systematically and exceedingly off-scale relative to pre-2013 data.

It is concluded that:

- There is no measurable warming or change in Rockhampton's climate.
- Identification of changepoints based on poorly researched and misleading metadata and application of arbitrary and inconsistent adjustments is neither credible nor scientific and should be abandoned.

Acknowledgements

Comments by David Mason-Jones, Ken Stewart and Geoff Sherrington were greatly appreciated.

Author's note: Although this draft paper has been carefully researched and uses statistical tools, data and other evidence that is available in the public domain, no responsibility is accepted for errors of fact arising from the scarcity of information or photographs etc.

Preferred citation:

Johnston, Bill 2020. Climate of the Great Barrier Reef, Queensland. Part 4. Climate change at Rockhampton. http://www.bomwatch.com.au/ 14 pp.

Figure 10. A progression of Queensland aerial photographs (cropped from QAP4142991 (1982); QAP4881134 (1990); QAP5222027 (1994); and QAP6040070 (2004)), showing developments at Rockhampton airport. 'X' marks the approximate location of the Stevenson screen after it moved from the Aeradio site in about 1956; CT, the 1960 control tower complex; S, SatCom equipment; AWS is the current (post 1994) site near the new met-office (mo). Estimated using Google Earth Pro, distance from the screen to the edge of pre-September 2003 hardstanding (h) was 30 m. Bare ground surrounding the post-1993 AWS site is due to the area being raised 1.5 m above natural ground level.

Appendix 1.

Aerodrome plan April 1941.

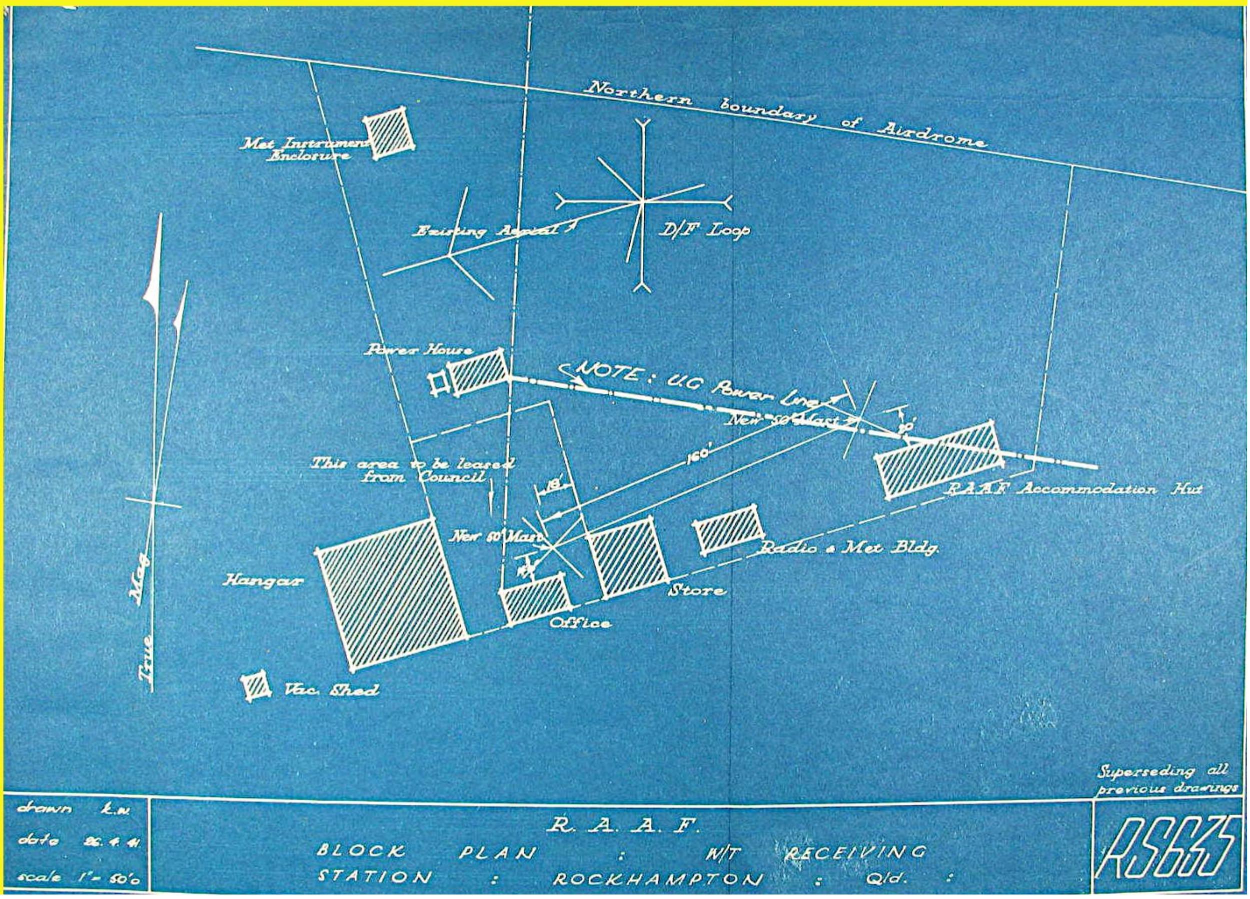

RAAF aerodrome plan April 1941 showing the Met. Instrument enclosure (upper left) and the Aeradio and meteorological office facing the apron (National Archives of Australia (NAA) Barcode 6678275).

Appendix 2

Tmax data used in the study.

Year	Rain	MaxAv	MaxN	MaxVar	MinAv	MinN	MinVar	SegmentDummy
1940	795.0	27.99	358	17.68	16.63	360	29.83	1
1941	612.0	27.73	365	17.91	15.81	365	35.43	1
1942	1178.5	28.36	364	18.37	16.89	362	21.78	1
1943	980.3	28.11	364	19.84	15.64	362	30.65	1
1944	620.8	28.23	362	19.49	15.59	364	30.76	1
1945	548.7	28.33	357	17.92	16.33	354	23.67	1
1946	636.3	29.11	363	14.25	15.17	363	42.76	1
1947	857.0	28.13	364	14.68	16.27	359	29.37	1
1948	517.0	28.64	363	18.65	15.87	364	28.66	1
1949	872.1	28.06	363	15.53	15.79	363	33.93	1
1950	1341.5	27.13	365	15.56	16.60	362	21.99	1
1951	714.9	28.77	364	18.61	15.14	365	33.16	1
1952	837.8	28.32	366	20.05	16.09	366	32.14	1
1953	836.2	28.25	365	15.52	15.44	363	36.34	1
1954	1162.2	27.58	365	16.01	16.81	364	21.17	1
1955	1450.6	27.83	364	17.05	16.51	365	25.09	1
1956	1617.2	27.37	366	20.68	15.70	365	36.41	1
1957	397.3	28.93	365	18.78	15.73	365	29.39	1
1958	944.0	28.42	365	16.58	16.54	365	29.29	1
1959	705.3	27.76	364	12.36	16.09	364	28.66	1
1960	808.8	27.66	366	17.57	15.04	366	37.59	1
1961	847.6	27.71	365	13.98	15.50	365	31.74	1
1962	644.2	28.71	365	17.32	16.17	365	30.65	1
1963	631.0	27.76	365	12.06	15.91	365	32.82	1
1964	720.2	28.35	366	18.06	16.85	364	29.71	1
1965	471.2	28.32	365	17.64	16.05	365	29.64	1
1966	619.4	27.84	365	16.04	15.92	365	27.37	1
1967	726.1	27.93	365	18.23	16.05	365	24.76	1
1968	1128.3	27.83	366	18.90	15.93	366	31.47	1
1969	639.6	28.43	365	17.01	16.98	365	26.22	1
1970	613.9	28.48	363	13.15	16.37	364	33.66	1
1971	1085.7	28.20	364	18.21	16.57	365	30.54	1
1972	599.2	28.50	365	14.21	15.90	366	29.64	1
1973	1631.0	28.22	365	14.12	18.11	364	20.06	1
1974	1172.3	27.83	365	14.06	16.03	365	34.07	1
1975	913.6	28.06	364	12.65	17.27	365	23.80	1
1976	995.4	27.90	366	14.22	16.79	366	34.13	1
1977	834.9	27.88	362	14.51	16.49	362	31.52	1
1978	1180.1	27.43	364	19.83	16.91	365	25.50	1
1979	470.0	28.46	365	15.72	16.87	365	27.64	1
1980	604.1	28.68	365	15.46	17.13	365	28.89	1
1981	711.8	27.98	364	16.38	16.90	364	29.24	1
1982	394.0	28.45	365	18.34	16.26	365	36.31	1
1983	1062.4	27.68	365	17.83	17.54	365	22.04	1
1984	698.0	27.84	366	15.14	16.60	366	26.99	1
1985	798.4	28.11	364	18.80	16.73	365	30.44	1
1986	781.6	28.20	365	17.91	17.00	365	24.46	1
1987	608.6	28.88	365	17.66	17.39	365	27.05	2
1988	1001.4	28.55	366	16.58	17.89	366	20.31	2
1989	1111.8	27.57	365	19.95	17.01	365	27.21	2
1990	1398.4	28.29	365	24.94	17.20	364	29.73	2
1991	797.4	28.96	365	13.28	17.16	365	30.16	2
1992	490.4	28.60	366	18.02	16.75	366	29.73	2
1993	589.6	28.56	364	14.34	17.51	364	16.86	2
1994	519.2	28.84	365	16.63	16.21	365	32.89	2
1995	785.4	28.71	365	19.99	17.35	365	27.34	2
1996	728.8	28.80	366	17.50	16.98	366	27.91	2
1997	541.4	28.29	365	17.52	17.06	365	23.73	2

1998	782.8	28.85	365	17.65	17.86	364	23.88	2
1999	531.0	28.51	365	13.07	16.62	365	25.76	2
2000	900.4	27.89	366	15.95	16.44	366	28.17	2
2001	525.8	29.35	365	15.40	17.08	365	27.40	2
2002	360.0	29.70	365	20.63	17.19	365	28.89	2
2003	705.6	29.04	365	13.09	17.58	365	22.55	2
2004	413.0	29.80	366	16.46	17.13	366	32.02	2
2005	634.0	29.48	365	19.76	17.66	365	24.87	2
2006	587.6	28.74	365	17.09	17.25	365	25.13	2
2007	681.2	28.45	365	20.10	17.22	365	28.33	2
2008	1087.2	28.17	366	15.79	16.79	366	27.97	2
2009	583.8	29.88	365	12.13	17.20	365	27.11	2
2010	1424.0	27.70	365	11.43	18.08	365	24.41	2
2011	901.6	27.91	365	14.29	16.78	365	32.42	2
2012	766.0	28.29	366	18.74	16.72	366	27.96	2
2013	1213.6	29.06	365	18.89	17.73	365	20.91	3
2014	1028.4	28.81	365	16.13	17.33	365	27.17	3
2015	682.8	29.39	365	14.34	17.57	365	25.91	3
2016	979.8	29.58	365	19.04	18.33	366	21.39	3
2017	832.2	29.68	365	14.23	18.17	365	23.57	3
2018	495.2	29.96	365	16.51	17.62	364	29.06	3
2019	295.8	30.12	365	18.26	17.62	365	28.43	3